

M.M. KULYK,<sup>1</sup> V.M. KALITA,<sup>1</sup> A.F. LOZENKO,<sup>1</sup> S.M. RYABCHENKO,<sup>1</sup>  
O.V. STOGNEI,<sup>2</sup> A.V. SITNIKOV<sup>2</sup>

<sup>1</sup>Institute of Physics, Nat. Acad. of Sci. of Ukraine  
(46, Nauky Ave., Kyiv 03680, Ukraine; e-mail: nikolaj.kulik.ifnasu@gmail.com)

<sup>2</sup>Voronezh State Technical University  
(14, Moscow Ave., Voronezh 394026, Russian Federation)

## IN-PLANE ANISOTROPY EFFECT ON CRITICAL TRANSITION FIELD IN NANOGRANULAR FILMS WITH PERPENDICULAR ANISOTROPY

PACS 75.70.Ak, 75.30.Gw,  
75.60.Ej, 62.23.Pq

*The influence of the in-plane anisotropy on the magnetization of a nanogranular film with perpendicular anisotropy has been studied. It is shown that if a magnetic field is tilted with respect to the film normal, a critical transition from the inhomogeneous magnetic state of granules with noncollinear directions of their moments to the homogeneous one with parallel orientation of granular magnetic moments takes place. The in-plane anisotropy is found to affect the angular dependence of the critical field. The ensemble of oriented biaxial particles is theoretically described in the double-well potential approximation. Despite the biaxial magnetic anisotropy of particles, their ensemble, if in the inhomogeneous state, is divided into two subensembles, with the magnetic moments of particles being collinear in each of them. In the critical field, a transition from the inhomogeneous state with two subensembles into the homogeneous one takes place. The results of theoretical calculations are compared with experimental data for a nanogranular Co/Al<sub>2</sub>O<sub>n</sub> film with perpendicular anisotropy containing 74.5 at.% Co, which exceeds the percolation threshold. The magnetic moment of this film is a sum of two contributions: from nanogranules with biaxial anisotropy and a phase forming the percolation cluster. The magnetic properties of nanogranules, whose contribution is separated from the total film magnetization, agree well with the calculation data.*

*Keywords:* in-plane anisotropy, nanogranular film, critical transition, double-well potential, percolation cluster, blocking temperature.

### 1. Introduction

Nanogranular magnetic films attract a keen interest owing to the prospects of their application in various functional devices [1–4], as well as because they are model objects for various problems of micromagnetism [5, 6]. There are two basic types of magnetic nanogranular (NG) composites: granules of a ferromagnetic (FM) metal in a nonmagnetic insulating matrix or FM granules in a nonmagnetic metal. In NG composites with a size of FM granules less than the critical one for the single-domain state [7, 8], the remagnetization of a granule occurs by means of the coherent rotation of the particle magnetization vector [9]. Below, we consider NG films of the type “single-domain FM metal granules

in the insulating matrix” without mentioning it every time.

For external magnetic fields lower than the uniaxial anisotropy one, the dependence of the magnetic energy of a granule on the orientation of its magnetic moment looks like a double-well potential [10, 11]. The magnetic moments of granules undergo thermally induced transitions between those wells [10, 11].

Describing the magnetic state of FM granules, an important concept is the blocking temperature,  $T_b$  [12]. Below  $T_b$ , the magnetic moment of the granule is “blocked” within a time interval of observation of the system. In this case, the probabilities of its orientation near each of two anisotropy energy minima do not correspond to the thermodynamic equilibrium and depend on the prehistory. As a result, the system demonstrates a hysteresis at the magnetization reversal [9, 13]. Above  $T_b$ , the thermodynamic

© M.M. KULYK, V.M. KALITA, A.F. LOZENKO,  
S.M. RYABCHENKO, O.V. STOGNEI,  
A.V. SITNIKOV, 2015

equilibrium for the populations of potential wells has enough time to be established during the observation period, and the hysteresis disappears [12,14]. The ensemble of particles transits into the superparamagnetic state.

However, as is shown in works [15–17], the directions of particles' magnetic moments in each of two minima of the double-well potential remain, to a great extent, localized close to these minima up to temperatures  $(3\div 4) T_b$ , though the ratio of “populations” of those minima are practically equilibrium [10]. The corresponding magnetic-field and temperature dependences of the ensemble magnetization deviate from the Langevin function [15,16]. The latter corresponding to the equiprobable orientation of the particles' magnetic moments into any direction in the absence of an external field. The direction distribution of magnetic moments in the film is not uniform in this case.

For a NG film with single-domain granules characterized by identical magnitudes of anisotropy perpendicular to the film plane, the emergence of a state with non-uniform distribution of magnetic moment directions can also be connected with another factor. The perpendicular anisotropy provides an energy minimum if the magnetic moments of granules are oriented normally to the film plane, whereas the anisotropy of the demagnetizing field, which is proportional to the normal film magnetization, dictates to the film the easy-plane anisotropy. In this case, the film magnetization in the field directed normally to the film plane and less by magnitude than a certain critical one,  $H_{\text{crit}}$ , gives rise to the emergence of an inhomogeneous state [10]. In this state, the magnetic moments of some FM granules are directed along the magnetic field, and those of other granules in the opposite direction. The demagnetization energy is lower, and the anisotropy energy has a minimum. At the magnetization of a film with perpendicular anisotropy of granules at an arbitrary angle  $\theta_H$ , the critical character of the transition between the homogeneous and inhomogeneous states survives [10]. The quantity  $H_{\text{crit}}$  depends on  $\theta_H$  in this case and it turns into zero at  $\theta_H = 90^\circ$ .

In the fields larger by magnitude than  $H_{\text{crit}}$ , the moments of all granules are oriented identically, and the whole system is in the homogeneous state [10]. However, at  $\theta_H \neq 0$ , the moments are not oriented along the external field: they are only tilted

with respect to it until the magnetization saturation is reached [10].

For the film as a whole, the field-induced transition between the states with homogeneous and inhomogeneous magnetizations is a phase transition of the order-disorder type [10, 18]. In the equilibrium case and at the normal magnetization,  $H_{\text{crit}}(\theta_H = 0)$  is equal to the largest possible field of film demagnetization,  $H_{d\text{max}} = 4\pi M_s$ . Here,  $\theta_H$  is the angle between the director for the magnetic field direction and the film normal ( $0 \leq \theta_H \leq \pi$ ),  $M_s$  is the saturation magnetization of the film as a whole ( $M_s = f_v M_{s\_gr}$ ),  $f_v$  is the volume fraction of the ferromagnetic material, of which granules are made, and  $M_{s\_gr}$  is the saturation magnetization of this material. The field  $H_{d\text{max}}$  is achieved when the magnetization is saturated by a normally oriented external field.

The state of a film with an inhomogeneous distribution of magnetic moment directions, which results from a competition between the perpendicular anisotropy and the demagnetization factor anisotropy, arises even at  $T = 0$ , without thermally induced transitions between the directions of magnetic moments in granules that correspond to the minima of the double-well potential. Just neglecting the thermally activated transitions, the “equilibrium magnetization” of films with perpendicular anisotropy was considered in work [10].

An acceptable approximation for the consideration of the system in this state is the model of two-level equilibrium system, which was used, e.g., in the consideration of the equilibrium magnetization in a nanogranular film with perpendicular anisotropy of particles [10]. In work [10], the behavior of the “equilibrium” (in the sense indicated above) magnetization of the films with perpendicular anisotropy of granules at various  $\theta_H$ 's and the dependences  $H_{\text{crit}}(\theta_H)$  for the isotropic in-plane films with  $f_v$  below the percolation threshold  $f_{vp}$  were considered. The results of work [10] were confirmed experimentally [19].

In a number of cases, NG films with perpendicular anisotropy can also have in-plane anisotropy. As far as we know, the regimes of magnetic reversal for nanogranular films with perpendicular and in-plane anisotropies have not been discussed in the literature.

As the volume fraction of granules in the film,  $f_v$ , grows, there arise small clusters, and when  $f_v$  reaches a value of  $f_{vp}$ , there appears a large percolation cluster penetrating throughout the film [20]. However,

even in this case, a considerable fraction of FM granules remain isolated. At the magnetic reversal, they have to demonstrate features typical of films with perpendicular anisotropy. The researches of an NG film with bi-phase magnetic content corresponding to the presence of non-percolating granules and a percolation granular cluster in the film were carried out in work [21]. In this paper, the issues concerning the resolution of contributions from those two groups of granules to the magnetization reversal curves and the features in the angular dependence of the coercive field in such film were discussed.

In this work, we report the results of our additional researches of a NG film  $\text{Co}/\text{Al}_2\text{O}_n$  with 74.5 at.% Co. This value should correspond to  $f_v \approx 0.79$ , which exceeds the percolation threshold. We also considered the transition between the homogeneous and inhomogeneous magnetization states of such bi-phase film. Besides the perpendicular anisotropy, the granular part of this film has the in-plane one as well [21]. The conditions for the critical transition in the granular part of the film from the state with homogeneous orientation of magnetic moments to the inhomogeneous one and their dependence on the direction of a magnetizing field in the biaxially anisotropic film are analyzed.

## 2. Experimental Part

### 2.1. Specimens and measurement methods

A batch of NG  $\text{Co}/\text{Al}_2\text{O}_n$  film specimens about  $5 \mu\text{m}$  in thickness was fabricated by the ion-beam sputtering of composite targets located at different ends of a long ( $25 \times 1 \text{ cm}^2$ ) sital substrate in the Ar atmosphere under a pressure of  $3.2 \times 10^{-5}$  Torr [18]. Such sputtering onto a long substrate was used in order to provide the same conditions while fabricating a set of films with various volume fractions of granules,  $f_v$ . After the film sputtering, the substrate was cut across into specimens: narrow strips with different Co contents. Therefore, the specimens were fabricated under the conditions of the inclined sputtering of components, especially the specimen with the minimum and maximum Co contents. In this case, the preferential direction in the film is the intersection of its plane with a plane formed by atomic beams. This direction corresponds to the narrow side of the specimen obtained after cutting the substrate. Let us designate it as  $Y$ . The direction along the long side of a

specimen is designated as  $X$ , and the direction normal to the specimen as  $Z$ . The dimensions of the examined sample of a film amounted to 10 and 2 mm along the  $X$  and  $Y$  sides, respectively. On the basis of the described procedure of film fabrication (the geometry of sputtering and the relative arrangement of the substrate and the targets), we may expect the manifestation of anisotropic effects in the film plane.

The electric percolation threshold, which was determined for this batch of films from the dependence of their electric resistance on the Co content [18], was found to equal 61 at.% Co, which should correspond to  $f_{vp} = 0.66$ . Films from this batch with Co contents from 45 to 75 at.% were studied earlier in work [22], and the film-growth-induced perpendicular magnetic anisotropy was found in them. It had the maximum magnitude near the percolation threshold. In work [23], the cross-section of a film from this batch with a Co content of 56 at.% was studied on a transmission electron microscope. It was shown that the granules with an average transverse size of about 4 nm are prolate along the direction of their growth, i.e. along the normal of the film. This fact explains the perpendicular anisotropy of the films, as a form anisotropy.

As was mentioned above, we study an NG  $\text{Co}/\text{Al}_2\text{O}_n$  film with 74.4 at.% Co ( $f_v \approx 0.79$ ), for which the percolation threshold is considerably exceeded. In the previous research [21], it was found that, in addition to the perpendicular magnetic anisotropy, this film also has in-plane anisotropy with the easy axis located in the film plane and oriented along the direction  $X$ . The electron microscopy research of the transverse cross-section of this film [21] showed that the specimen included both percolating clusters and non-percolating granules, and the relative fraction of the latter dominated. The research of a magnetic contrast on an atomic force microscope [21] revealed that, at room temperature, the specimen had a stripe domain structure with the average domain width being about  $1 \mu\text{m}$ . The prevailing direction of the domain stripes in the absence of an external field coincided with the axis  $X$ . Hence, at room temperature, the examined film was in the superferromagnetic state (a state with the ferromagnetic ordering of superparamagnetic granules, which were separated from one another, owing to the magnetic interaction between them).

The measurements of magnetization reversal curves were carried out on a vibrating-sample magnetometer LDJ-9500 at room temperature.

## 2.2. Results of measurements

The families of magnetization reversal loops were registered at various directions of the introduction of an external magnetic field into the film, with  $0 \leq \theta_H \leq 90^\circ$  in the specimen planes  $XZ$  ( $\varphi_H = 0$ ) and  $YZ$  ( $\varphi_H = 90^\circ$ ), which are shown in Fig. 1. Hereafter,  $\theta_H$  ( $0 \leq \theta_H \leq 180^\circ$ ) is the angle between the direction of the conditionally selected positive direction of the film normal and external magnetic field director (the slope angle of the axis, along which the magnetic field  $H$ ). Under such definition of the field direction, the field itself can be considered as changing from  $+\infty$  to  $-\infty$  at a constant  $\theta_H$  in the spherical coordinate system used for calculations. The angle  $\theta_H$  between the vector of the external magnetic field strength  $\mathbf{H}$  and the “positive” direction of the film normal depends in this case on the field sign:  $\theta_H = \theta_H + [1 - \text{sign}(H)]\pi/2$ , where  $\text{sign}(x) = 1, 0$ , and  $-1$  for  $x > 0, x = 0$ , and  $x < 0$ , respectively. Accordingly, the azimuthal angle  $\varphi_H$  for the direction of the magnetic field vector should be defined as  $\varphi_H = \varphi_H + [1 - \text{sign}(H)]\pi/2$ . Here,  $\varphi_H$  is the azimuthal angle of the director for the external magnetic field in the upper hemisphere. The angle  $\varphi_H$  is reckoned from the positive direction of the axis  $X$ .

The curves shown in Fig. 1 correspond to those expected for ferromagnetic films with perpendicular and in-plane anisotropies and a magnitude of  $4\pi M_s$  for the maximum demagnetizing, which is much larger than the fields of perpendicular ( $H_{A\theta}$ ) and in-plane ( $H_{A\varphi}$ ) magnetic anisotropies of the film.

The hysteresis reveals itself unusually in the registered curves. It is concentrated in a small part of magnetization reversal curves, at low fields (see the insets in Fig. 1). In work [21], it was shown that those hysteresis sections are the manifestations of the contribution made by the percolating part of the examined film to the magnetization reversal curve. The percolating part feels the action of an internal field associated with the dominating contribution of non-percolating granules to the film magnetization. This internal field equals the vector sum of the external and demagnetizing fields. The latter has only a  $Z$ -component directed opposite to the  $Z$ -component of an external field. The perpendicular anisotropy of FM

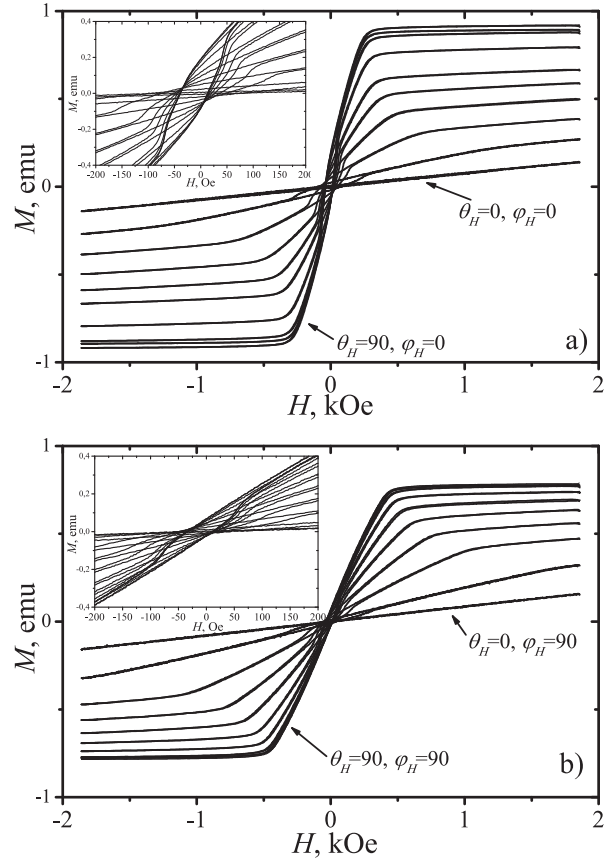


**Fig. 1.** Magnetization reversal loops for magnetic field orientations in planes (a)  $XZ$ , which corresponds to  $\varphi_H = 0$ , and (b)  $YZ$ , which corresponds to  $\varphi_H = 90^\circ$ . Loops were measured with an angle increment of  $10^\circ$ . The scaled-up fragments of central loop sections are shown in the insets

granules results in that the demagnetization almost completely compensates the projection of an external field onto the axis  $Z$  if the field is lower than the critical one [10]. At the same time, the contribution of the percolating part of the film is responsible for both the coercive field and its unusual angular dependence, which was analyzed in work [21].

If we neglect the hysteresis in the narrow region of low fields, then, in the field intervals between rather sharp transitions to the saturation, the position of which depends on  $\theta_H$ , and  $\varphi_H$ , the film magnetization is a linear function of the field. Such a behavior almost corresponds to the model of equilibrium magnetization reversal in a tilted magnetic field for the film with perpendicular anisotropy, which was considered in works [10, 19]. The only difference consists in that

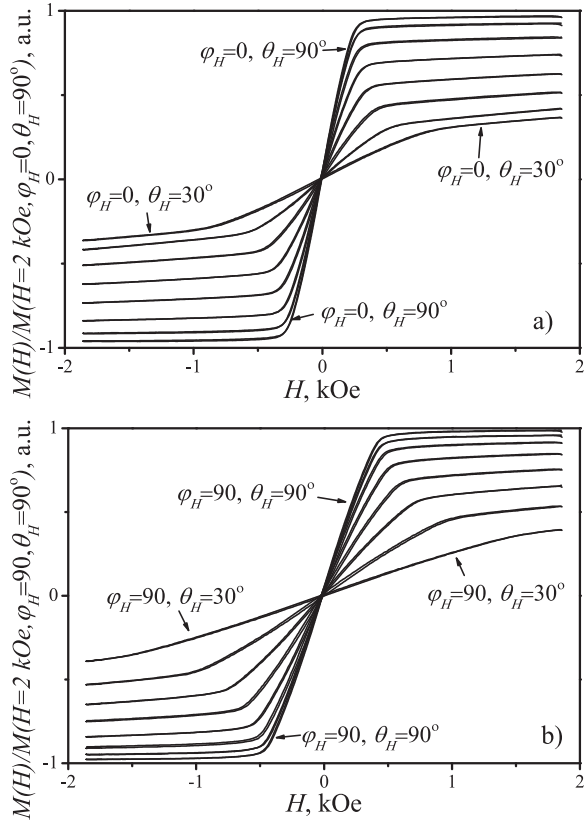


**Fig. 2.** Resolved granular contributions to the magnetization reversal loop of NG Co/Al<sub>2</sub>O<sub>n</sub> film for various angles within the interval  $30^\circ \leq \theta_H \leq 90^\circ$  and  $\mathbf{H}$  in the planes XZ (a) and YZ (b)

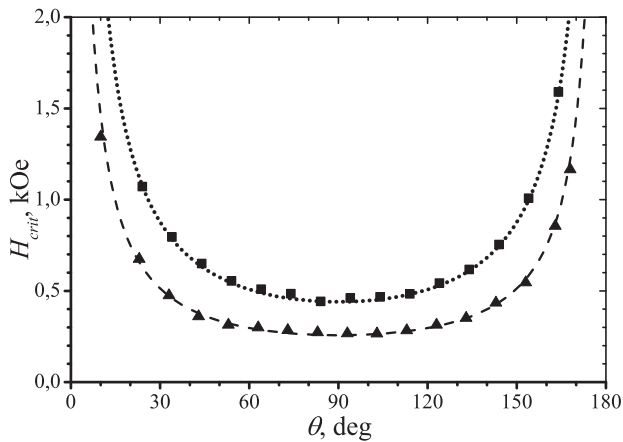


**Fig. 3.** Experimental dependences  $H_{\text{crit}}(\theta_H)$  for the external field in the planes YZ ( $\varphi_H = 90^\circ$ , ■) and XZ ( $\varphi_H = 0^\circ$ , ▲). The curves correspond to the approximation of experimental dependences at  $\varphi_H = 90^\circ$  and  $0^\circ$  by expressions (17) and (18), respectively

the fields of the sharp inflection to saturation in the dependences  $M_H(\theta_H)$  are different for the field direction planes XZ and YZ. In nanogranular films with perpendicular anisotropy, those fields of the sharp inflection to saturation are critical, i.e. the equilibrium inhomogeneous ensemble of granules transforms in them into the equilibrium homogeneous one [10].

In work [21], we proposed a method to resolve the obtained magnetization reversal curves into components given by the “granular” and “percolating” parts of the film with the use of the derivatives of magnetization reversal curves. Since the aim of the present work is to analyze the dependences of critical fields, at which the granular part of the film transits from the equilibrium inhomogeneous state of the ensemble of granules into the equilibrium homogeneous one, only the granular contribution to the magnetization reversal curves resolved using the method proposed in work [21] will be considered in what follows.

The normalized magnetization reversal loops for this contribution are shown in Fig. 2, a, b for the field direction planes XZ and YZ, correspondingly. It should be noted that, at  $\theta_H < 30^\circ$ , the sharp inflections in the curves shift toward larger fields, and the approach to the saturation level after it becomes very slow, which is associated with a large value of  $4\pi M_s$  for the film concerned. Therefore, the curves for those angles were not plotted in Fig. 2. In both a and b cases, all curves demonstrate a behavior typical of NG films with perpendicular anisotropy at “equilibrium” (in the sense discussed in Introduction): an almost linear  $M(H)$ -dependence, free of hysteresis, in low fields; then a sharp inflection and a smooth asymptotic approach to the saturation level at high fields. Both the slope angle of the linear section and the position of the critical transition point (the inflection point) have their own angular dependences. It should also be noted that the slope angle of the linear section at low fields in the dependence  $M(H)$  in Fig. 2, a differs insignificantly from that in Fig. 2, b. Additionally, the dashed curves in Fig. 3 approximate the dependences  $H_{\text{crit}}(\theta_H)$  by expressions, which are derived in the next section.

### 3. Model

As was mentioned above, in work [10], the magnetization reversal in an arbitrarily directed external field and the critical transition from the state with ho-

mogeneous magnetization to the state with different orientations of magnetic moments in two subensembles of FM granules were considered for a NG film, which is isotropic in its plane, but with perpendicular anisotropy, and with the volume fraction occupied by granules,  $f_{\text{gr}}$ , below the percolation threshold. That is, the volume fraction of a FM material in the film,  $f_v$ , was considered to equal  $f_{\text{gr}}$ . From the discussion of experimental data, it follows that two factors in the case considered in this work are different. First, the examined film is above the percolation threshold, i.e.  $f_v > f_{vp}$  for it, so that it consists of “granular”  $f_{\text{gr}} < f_v$  and “percolating” parts. Second, besides the perpendicular anisotropy, this film is also characterized by the in-plane one. Let us consider how those differences can be taken into account on the whole in the framework of the approach used in works [10, 21].

### 3.1. Role of the overpercolating state of a film and its account

In order to consider the overpercolating state of a film, let us introduce the relative volume of a FM metal in the composite, which consists of the separate granules,  $f_{\text{gr}}$ , and the relative volume of this material in the percolation cluster,  $f_{\text{per}}$ . Then  $f_v = f_{\text{gr}} + f_{\text{per}}$ .

In this subsection, for simplification, we neglect the in-plane anisotropy. Since we consider the equilibrium (in the sense described in Introduction) state of the film, we may confine the consideration to the interval of magnetic fields  $H > 0$  and select the reference point for the angle  $\varphi$  so that  $\varphi_{\text{H}} = 0$ . Then, at a field larger than the critical one, when the magnetic moments of all granules are oriented identically, the magnetic energy density in the two-component system consisting of granules with perpendicular anisotropy and the percolating part looks like

$$\begin{aligned}
 U = & -f_{\text{gr}}Kj^2 \cos^2 \theta_{\text{gr}} + \\
 & + \frac{1}{2}N_{zz}(f_{\text{gr}}j \cos \theta_{\text{gr}} + f_{\text{per}}j \cos \theta_{\text{per}})^2 - \\
 & - H(\cos \theta_{\text{H}}(f_{\text{gr}}j \cos \theta_{\text{gr}} + f_{\text{per}}j \cos \theta_{\text{per}}) + \\
 & + \sin \theta_{\text{H}}(f_{\text{gr}}j \sin \theta_{\text{gr}} + f_{\text{per}}j \sin \theta_{\text{per}})). \quad (1)
 \end{aligned}$$

Here, the first term describes the contribution to the energy from the uniaxial anisotropy of the non-percolating part of granules ( $K > 0$  is the anisotropy constant for the non-percolating part of granules), the

second term is the demagnetization energy ( $N_{zz}$  is the demagnetizing factor), and the third term is the Zeeman contribution. The angles of the magnetic moment directions of granules,  $\theta_{\text{gr}}$ , and the percolating part,  $\theta_{\text{per}}$ , are not identical. The filling factors of the film with granules,  $f_{\text{gr}}$ , and with the percolating part,  $f_{\text{per}}$ , were also taken into account. The absolute values of their own magnetizations,  $j$ , were adopted to be equal.

The equation for the extremes of the energy density for a two-component system in the state where the magnetic moments of granules are directed identically can be obtained by differentiating Eq. (1) with respect to the angles and equating the derivatives to zero,

$$\begin{aligned}
 \frac{\partial U}{\partial \theta_{\text{gr}}} = & 2f_{\text{gr}}Kj^2 \cos \theta_{\text{gr}} \sin \theta_{\text{gr}} - \\
 & - N_{zz}f_{\text{gr}}j^2(f_{\text{gr}} \cos \theta_{\text{gr}} + f_{\text{per}} \cos \theta_{\text{per}}) \sin \theta_{\text{gr}} - \\
 & - Hf_{\text{gr}}j(-\cos \theta_{\text{H}} \sin \theta_{\text{gr}} + \sin \theta_{\text{H}} \cos \theta_{\text{gr}}) = 0, \quad (2)
 \end{aligned}$$

$$\begin{aligned}
 \frac{\partial U}{\partial \theta_{\text{per}}} = & -N_{zz}f_{\text{per}}j^2(f_{\text{gr}} \cos \theta_{\text{gr}} + f_{\text{per}} \cos \theta_{\text{per}}) \sin \theta_{\text{per}} - \\
 & - Hf_{\text{per}}j(-\cos \theta_{\text{H}} \sin \theta_{\text{per}} + \sin \theta_{\text{H}} \cos \theta_{\text{per}}) = 0. \quad (3)
 \end{aligned}$$

Let us consider a state of the system, in which the demagnetizing field is compensated by the  $Z$ -projection of the external magnetic field. This is the lowest value of external field, at which the magnetic moments of all granules still remain oriented identically. Let us define it as “critical”:

$$N_{zz}j(f_{\text{gr}} \cos \theta_{\text{gr}} + f_{\text{per}} \cos \theta_{\text{per}}) - H_{\text{crit}} \cos \theta_{\text{H}} = 0. \quad (4)$$

Substituting Eq. (4) into Eqs. (2) and (3) allows us to find the external field for this critical point and the corresponding magnetization orientations  $\theta_{\text{gr}}^{(\text{cr})}$  and  $\theta_{\text{per}}^{(\text{cr})}$ . Note that earlier, in work [10], the critical field for the film with perpendicular anisotropy of granules with  $f_v < f_{vp}$  was defined as the limiting case for the state, in which the granules form two subensembles.

From Eqs. (2), (3), and (4), we obtain that the following conditions are satisfied at the critical point:

$$\begin{aligned}
 N_{zz} = & f_{\text{gr}}j \cos \theta_{\text{gr}}^{(\text{cr})} - H_{\text{cr}} \cos \theta_{\text{H}} = 0, \\
 2f_{\text{gr}}Kj \sin \theta_{\text{gr}}^{(\text{cr})} - & H_{\text{cr}} \sin \theta_{\text{H}} = 0, \quad \cos \theta_{\text{per}}^{(\text{cr})} = 0. \quad (5)
 \end{aligned}$$

While comparing Eqs. (5) with the corresponding equations in work [10], one can see that the former

give the same values for the critical field in the case  $f_v < f_{vp}$ ; now, the equations include the relative volume of non-percolating granules,  $f_{gr}$ , rather than the whole relative volume of a ferromagnetic substance in the NG film. In the non-percolating film, which was considered in work [10], those two quantities were identical.

The solution of Eqs. (2) and (3) makes it possible to find the required dependences for the projection of the magnetic moment of a percolating film onto the external field if the latter exceeds the critical value ( $|\mathbf{H}| > H_{crit}$ ). Below the critical point ( $|\mathbf{H}| < H_{crit}$ ), the magnetic moments of granules in the film are not oriented identically, which diminishes the positive demagnetization energy, but keeps the gain provided by the anisotropy energy, as was described in work [10].

### 3.2. Biaxial anisotropy

The description of the critical transition induced by a magnetic field in the NG film with perpendicular anisotropy of granules between the state with uniformly oriented magnetic moments of all granules and the state with their non-uniform orientation, which was used in work [10], was based on the model that, in the fields with  $|\mathbf{H}| < H_{crit}$ , there exist two subensembles of granules with different average orientations of magnetic moments in the film. As a result, the positive energy of demagnetization becomes lower, but the gain in the negative energy of perpendicular anisotropy is preserved. The relative numbers of granules related to either of the subensembles are denoted as  $p_1$  and  $p_2$  ( $p_1 + p_2 = 1$ ). The states with homogeneous magnetization at  $|\mathbf{H}| > H_{crit}$  correspond to the combination  $p_1 = 1$  and  $p_2 = 0$  (at  $H > H_{crit}$ ) or the combination  $p_1 = 0$  and  $p_2 = 1$  (at  $-H < -H_{crit}$ ).

Let us use a similar approach in the case where the granular part of a film has both perpendicular and in-plane anisotropies. On the basis of the consideration in Section 3.3.1, we analyze only the contribution of the granular part, taking into account that the relative volume occupied by non-percolating granules in the film equals  $f_{gr} = f_v - f_{per}$ . We also confine the consideration to the case  $H > 0$ . Taking the indicated factors into account, the equation for the total magnetic energy in the granular part reads

$$U_{tot} = f_{gr} \{-K_\theta(p_1 \cos^2 \theta_1 + p_2 \cos^2 \theta_2) + K_\varphi(p_1 \cos^2 \varphi_1 \sin^2 \theta_1 + p_2 \cos^2 \varphi_2 \sin^2 \theta_2) +$$

$$+ \frac{1}{2} N_{zz} f_{gr} j^2 (p_1 \cos \theta_1 + p_2 \cos \theta_2)^2 - H j [(p_1 \cos \theta_1 + p_2 \cos \theta_2) \cos \theta_H + (p_1 \cos(\varphi_1 - \varphi_H) \sin \theta_1 + p_2 \cos(\varphi_2 - \varphi_H) \sin \theta_2) \sin \theta_H]\}. \quad (6)$$

Here,  $U_{tot}$  is the total energy density in the granular part,  $j$  the magnetic moment of a granule,  $K_\theta$  the perpendicular anisotropy constant,  $K_\varphi$  the in-plane anisotropy constant,  $\theta_1, \theta_2, \varphi_1$ , and  $\varphi_2$  are the angles of magnetic moment directions of granules in the subensembles measured in spherical coordinates, and  $\theta_H$  and  $\varphi_H$  are the director tilt angles for the external magnetic field  $H$ . For simplification, let us introduce the quantity  $\Delta p = p_1 - p_2$ . Then,  $p_1 = \frac{1+\Delta p}{2}$  and  $p_2 = \frac{1-\Delta p}{2}$ . The extremes of  $U_{tot}$  with respect to the parameters  $\theta_1, \theta_2, \varphi_1, \varphi_2$ , and  $\Delta p$  can be found by equating the corresponding derivatives to zero:

$$\begin{aligned} \frac{\partial U_{tot}}{\partial \theta_1} = f_{gr} \{ & (1 + \Delta p) K_\theta \cos \theta_1 \sin \theta_1 + \\ & + (1 + \Delta p) K_\varphi \cos \varphi_1 \cos^2 \varphi_1 \sin \theta_1 - \\ & - \frac{1}{4} f_{gr} j^2 N_{zz} ((1 + \Delta p) \cos \theta_1 + \\ & + (1 - \Delta p) \cos \theta_2) (1 + \Delta p) \sin \theta_1 - \\ & - \frac{1}{4} H j (1 + \Delta p) (\cos \theta_1 \cos(\theta_1 - \theta_H) \sin \theta_H - \\ & - \cos \theta_H \sin \theta_1) \} = 0, \end{aligned} \quad (7)$$

$$\begin{aligned} \frac{\partial U_{tot}}{\partial \theta_2} = f_{gr} \{ & (1 - \Delta p) K_\theta \cos \theta_2 \sin \theta_2 + \\ & + (1 - \Delta p) K_\varphi j \cos \theta_2 \cos^2 \varphi_2 \sin \theta_2 - \\ & - \frac{1}{4} (1 - \Delta p) f_{gr} j^2 N_{zz} ((1 + \Delta p) \cos \theta_1 + \\ & + (1 - \Delta p) \cos \theta_2) \sin \theta_2 + \\ & + \frac{1}{2} (1 - \Delta p) H j \cos \theta_H \sin \theta_2 \} = 0, \end{aligned} \quad (8)$$

$$\begin{aligned} \frac{\partial U_{tot}}{\partial \varphi_1} = f_{gr} \{ & -(1 + \Delta p) K_\varphi j \cos \varphi_1 \sin^2 \theta_1 \sin \varphi_1 + \\ & + \frac{1}{2} (1 + \Delta p) H j \sin \theta_1 \sin \theta_H \sin(\varphi_1 - \varphi_H) \} = 0, \end{aligned} \quad (9)$$

$$\frac{\partial U_{\text{tot}}}{\partial \varphi_2} = f_{\text{gr}} \{ -(1 - \Delta p) K_{\varphi} \cos \varphi_2 \sin^2 \theta_2 \sin \varphi_2 + \frac{1}{2} (1 - \Delta p) H j \sin^2 \theta_{\text{H}} \sin(\varphi_2 - \varphi_{\text{H}}) \} = 0, \quad (10)$$

$$\begin{aligned} \frac{\partial U_{\text{tot}}}{\partial \Delta p} = f_{\text{gr}} \left\{ -\frac{1}{2} K_{\theta} (\cos^2 \theta_1 - \cos^2 \theta_2) + \frac{1}{2} K_{\varphi} (\cos^2 \varphi_1 \sin^2 \theta_1 - \cos^2 \varphi_2 \sin^2 \theta_2) + \frac{1}{4} f_{\text{gr}} j^2 N_{zz} (\cos \theta_1 - \cos \theta_2) ((1 + \Delta p) \times \right. \\ \left. \times \cos \theta_1 + (1 - \Delta p) \cos \theta_2) - \frac{1}{2} H j ((\cos \theta_1 - \cos \theta_2) \cos \theta_{\text{H}} + \sin \theta_{\text{H}} (\cos(\varphi_1 - \varphi_{\text{H}}) \times \right. \\ \left. \times \sin \theta_1 - \cos(\varphi_2 - \varphi_{\text{H}}) \sin \theta_{\text{H}})) \right\} = 0. \quad (11) \end{aligned}$$

From the system of equations (7), (8), and (11), it follows that, in the equilibrium state with  $|\Delta p| \neq 1$ ,

$$\theta_1 + \theta_2 = 180^\circ. \quad (12)$$

The solution of the system of equations (7)–(11) for an arbitrary angle  $\varphi_{\text{H}}$  is rather complicated even in the numerical form. Therefore, let us consider only two cases:  $\varphi_{\text{H}} = 0$  and  $90^\circ$ . From Eqs. (9) and (10), one can see that, in those cases, the condition  $\varphi_1 = \varphi_2 = \varphi_{\text{H}}$  is satisfied. For convenience, let us introduce the anisotropy fields and the maximum possible demagnetizing field created by the granular part of the film ( $\Delta p = 0$  or  $1$  if  $\theta_{\text{H}} = 0$ ), by using the substitutions  $H_{a\theta} = \frac{2K_{\theta}}{j}$ ,  $H_{a\varphi} = \frac{2K_{\varphi}}{j}$ , and  $H_d^{\text{max}} = j f_{\text{gr}} N_{zz}$ .

In the fields below the critical one, the state of equilibrium inhomogeneous magnetization is realized. With regard for expression (12), let us solve the system of equations (2) and (6) in the cases where  $\varphi_{\text{H}} = 0$  and  $90^\circ$ . For the system in the equilibrium inhomogeneous state, the parameters  $\Delta p$  and  $\theta_1$  look as follows:

if  $\varphi_{\text{H}} = 0$ ,

$$\theta_1(\varphi_{\text{H}} = 0) = \arcsin \left( \frac{H \sin \theta_{\text{H}}}{H_{a\theta} - H_{a\varphi}} \right), \quad (13)$$

$$\Delta p(\varphi_{\text{H}} = 0) = \frac{H \cos \theta_{\text{H}}}{H_d^{\text{max}} \sqrt{1 - \frac{H^2 \sin^2 \theta_{\text{H}}}{(H_{a\theta} - H_{a\varphi})^2}}}, \quad (14)$$

if  $\varphi_{\text{H}} = 90^\circ$ ,

$$\theta_1(\varphi_{\text{H}} = 90^\circ) = \arcsin \left( \frac{H \sin \theta_{\text{H}}}{H_{a\theta}} \right) \quad (15)$$

$$\Delta p(\varphi_{\text{H}} = 90^\circ) = \frac{H \cos \theta_{\text{H}}}{H_d^{\text{max}} \sqrt{1 - \frac{H^2 \sin^2 \theta_{\text{H}}}{H_{a\theta}^2}}}. \quad (16)$$

At the critical transition point,  $|\Delta p|$  becomes equal to 1, and two subensembles merge into one. From expressions (14) and (16), we find the critical field magnitude:

if  $\varphi_{\text{H}} = 0$ ,

$$\begin{aligned} H_{\text{crit}}(\varphi_{\text{H}} = 0) = \\ = \frac{(H_{a\theta} - H_{a\varphi}) H_d^{\text{max}}}{\sqrt{(H_{a\theta} - H_{a\varphi})^2 \cos^2 \theta_{\text{H}} + (H_d^{\text{max}})^2 \sin^2 \theta_{\text{H}}}}, \quad (17) \end{aligned}$$

if  $\varphi_{\text{H}} = 90^\circ$ ,

$$H_{\text{crit}}(\varphi_{\text{H}} = 90^\circ) = \frac{H_{a\theta} H_d^{\text{max}}}{\sqrt{H_{a\theta}^2 \cos^2 \theta_{\text{H}} + (H_d^{\text{max}})^2 \sin^2 \theta_{\text{H}}}}. \quad (18)$$

In the case where  $H \geq H_{\text{crit}}$ , the system of superparamagnetic granules transits into the homogeneously magnetized state, which is characterized by the parameters  $|\Delta p| = 1$  and  $\theta_1 = \theta_2 = \theta_m$ . However, bearing in mind that the system also contains the percolating part, the contribution of the latter to the demagnetizing field has to be taken into account. Neglecting this contribution in the case of a non-percolating film with perpendicular and in-plane anisotropies, the derivative of  $U_{\text{tot}}$  with respect to  $\theta_{\text{crit}}$  for the homogeneously magnetized system looks as follows:

if  $\varphi_{\text{H}} = 0$ ,

$$\begin{aligned} \frac{\partial U_{\text{tot}}}{\partial \theta_m} = H j \cos \theta_{\text{H}} \sin \theta_m - j \cos \theta_m (H \sin \theta_{\text{H}} + \\ + (-H_{a\theta} + H_{a\varphi} + H_d^{\text{max}}) \sin \theta_m), \quad (19) \end{aligned}$$

if  $\varphi_{\text{H}} = 90^\circ$ ,

$$\begin{aligned} \frac{\partial U_{\text{tot}}}{\partial \theta_m} = -j (H \sin(\theta_{\text{H}} - \theta_m) + \\ + H_d^{\text{max}} \cos \theta_m \sin \theta_m) + \frac{j}{2} H_{a\theta} \sin(2\theta_m). \quad (20) \end{aligned}$$

One can obtain the equations for the equilibrium values of  $\theta_m$  by equating (19) and (20) to zero.



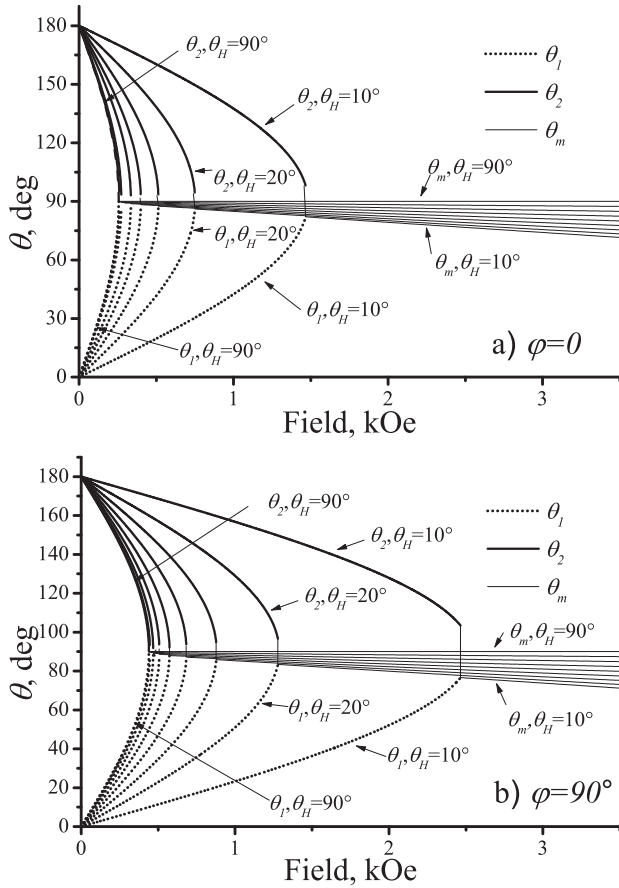


**Fig. 4.** Dependences of magnetization orientations for the subensembles of NG particles on the external magnetic field for various  $\theta_H$ : (a)  $\varphi_H = 0$  and (b)  $\varphi_H = 90^\circ$

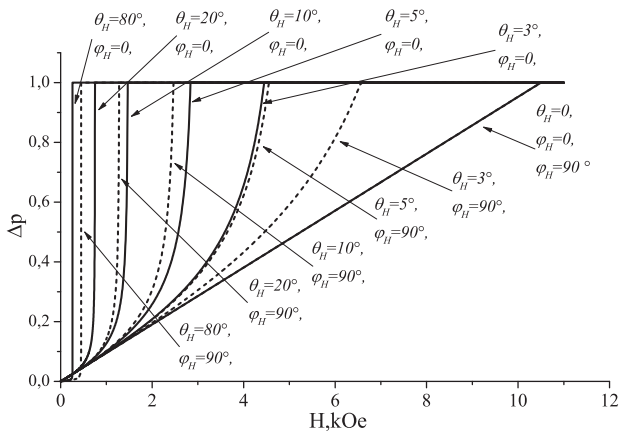


**Fig. 5.** Population difference  $\Delta p$  at the magnetization in various directions within the interval  $0^\circ \leq \theta_H \leq 90^\circ$  (an increment of  $10^\circ$ ) for two planes of the magnetic field orientations: with  $\varphi_H = 0$  (solid curves) and with  $\varphi_H = 90^\circ$  (dashed curves)

#### 4. Comparison of the Model with the Experiment

By approximating the experimental data obtained for the dependence  $H_{crit}(\theta_H)$  in the cases where the external field is located in the planes  $YZ$  ( $\varphi_H = 90^\circ$ ) and  $XZ$  ( $\varphi_H = 0$ ) (see Fig. 3), we determined the values  $H_d^{max} = 10.5 \pm 0.5$  kOe,  $H_{a\theta} = 0.44 \pm 0.02$  kOe, and  $H_{a\varphi} = 0.183 \pm 0.02$  kOe. The equilibrium dependences for  $\theta_1$ ,  $\theta_2$  and  $\theta_m$ , which are described by Eqs. (13) and (15), were calculated for the indicated values; they are depicted in Fig. 4 for the external magnetic field orientations in the planes that contain the normal to the film and the easy (Fig. 4, a) or hard (Fig. 4, b) axis of the in-plane anisotropy. Since, according to the estimations carried out in work [21], the contribution made by the percolating part of the film to its magnetization in the saturated state does not exceed 20%, the quantity  $\theta_m$  was calculated by equating derivatives (19) and (20) to zero and neglecting this contribution. In the inhomogeneous state, the moments of both subensembles deflect toward the equilibrium direction almost linearly, with a drastic ultimate transition into the homogeneous state; afterward, the direction of the magnetic moments in the single, united ensemble with  $\Delta p = 1$  asymptotically approaches the direction of  $\mathbf{H}$ . The difference from the corresponding solutions obtained in work [10] mainly consists in the difference between the dependences  $\theta_1(H_e)$  and  $\theta_2(H_e)$  for various  $\varphi_H$ .

In Fig. 5, the difference between the populations in both subensembles,  $\Delta p$ , in the region of states with inhomogeneous magnetization is shown. It was calculated, by using Eqs. (14) and (16).

In Figs. 4 and 5, one can clearly see the critical transition points. In Fig. 4, these are collapses of two subensembles with the different directions  $\theta_1$  and  $\theta_2$  into a single ensemble with the direction  $\theta_m$ . This collapse is the most pronounced in the case  $\theta_H = 10^\circ$ ; for other angles, the collapse region narrows and becomes not so appreciable. In Fig. 5, the change  $\Delta p$  for two subensembles is rather smooth at small non-zero  $\theta_H$ -angles. However, already at  $\theta_H > 10^\circ$ , the quantity  $\Delta p$  demonstrates a rather strong inflection to the state with  $\Delta p = \pm 1$  at fields close to the critical one depending on  $\theta_H$ . Figure 3 testifies to the agreement between the experimental values of critical field and those calculated with the values of  $H_d^{max}$ ,  $H_{a\theta}$ , and  $H_{a\varphi}$  indicated above. As follows from Figs. 4 and 5,

the values of critical transition field obtained with the same values of  $H_d^{\max}$ ,  $H_{a\theta}$ , and  $H_{a\varphi}$  are in good numerical agreement with the experimental data shown in Fig. 3.

As to the external field orientation  $\theta_H = 0$  (not exhibited in Fig. 4), we obtain  $\theta_1 = 0$  and  $\theta_2 = 180^\circ$  in this case up to  $H_d^{\max}$ . At  $H = H_d^{\max}$ , the system transits into a homogeneously magnetized state, and  $\theta_m = 0$ . In this configuration, the directions of grain magnetic moments in the subensembles do not change with the field. Only the populations of the subensembles change without any deflection of their moments. From Fig. 5, it is evident that, for the orientation  $\theta_H = 0$ , the dependence  $\Delta p(H)$  is completely linear at both  $\varphi_H$ -values. It saturates at the field equal to the maximum demagnetizing field  $H_d^{\max}$ . At other orientations different from  $\theta_H = 0$ , the quantity  $\Delta p$  grows firstly rather slowly in low fields; then, approaching  $H_{\text{crit}}$ , a drastic increase to  $\Delta p = 1$  takes place.

As is seen from Figs. 4 and 5, the presence of the in-plane anisotropy together with the perpendicular one leads to a relative shift of the transition points into the homogeneous state for the magnetic field lying in the same plane with the easy or hard axis of the in-plane anisotropy and the film normal. The value of this shift depends from  $\theta_H$ . It is absent at  $\theta_H = 0$ , reaches maximum at intermediate values of  $\theta_H$ , and is equal to  $H_{a\theta} - H_{a\varphi}$  at  $\theta_H = 90^\circ$ .

If the film has only perpendicular anisotropy (it consists of uniaxial granules), any in-plane direction is hard. However, if the anisotropy has also the in-plane component (if the granules are biaxial), and if the field  $H$  is applied along the easy axis of this anisotropy, the transition through the critical point into the homogeneous state will take place faster than in the former case.

Besides the critical transition field, the in-plane anisotropy also affects the magnetic susceptibility of granules in low fields, i.e. the slope of the curve of the granular contribution to the dependence  $M(H)$  at such fields (see Fig. 2). From Fig. 6, one can see how the  $\theta_H$ -dependence of the susceptibility – it is obtained at small fields as the normalized derivative

$$\chi_{\text{norm}} = \left. \frac{\partial (M/M_s)}{\partial (H/H_{a\theta})} \right|_{H \rightarrow 0}$$

– is modified, by depending on the direction of the external magnetic field projection on the film plane with

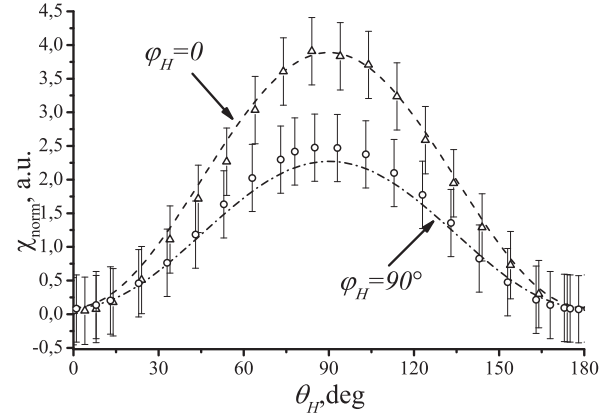


**Fig. 6.** Comparison between the low-field susceptibilities measured experimentally (symbols) and the results of model calculations (curves):  $\varphi_H = 0$  (triangles and dashed curve) and  $\varphi_H = 90^\circ$  (circles and dash-dotted curve)

respect to the easy axis of the in-plane anisotropy. In Fig. 6, the symbols correspond to experimental data, whereas the curves to the results of theoretical calculations, with the values of  $H_{a\theta}$ ,  $H_{a\varphi}$  and  $H_d^{\max}$  being obtained from the results of approximation of the  $H_{\text{crit}}$  angular dependences (the position of the critical transition) given above. It is possible to say about quite a good correspondence between the model and the experiment.

## 5. Conclusions

In works [10, 19], a model for the description of “equilibrium” dependences  $M(H_e)$  for NG films with perpendicular anisotropy in a tilted external magnetic field was considered. It was verified there for the ratio  $H_d^{\max}/H_a = 3$  and compared with the experiment for the ratio equal to 4.3. In this work, this model is compared with the experiment for the ratios  $H_d^{\max}/H_{a\theta} \approx 24$  and  $H_d^{\max}/(H_{a\theta} - H_{a\varphi}) \approx 41$ . The comparison results testify that the given model is valid in a wide interval of values of this ratio. Naturally, for practical applications of granular films with perpendicular anisotropy, the materials, for which this ratio is less than 1, are of high importance. The model has no restrictions with respect to the values of indicated ratio.

The model concerned is developed and compared with the experimental data obtained for a NG film which, in addition to the perpendicular anisotropy of granules, also has in-plane anisotropy. Analytical expressions in the case of a tilted external field are derived for the magnetization oriented in planes that

contain the normal to the film and the easy or hard axis of the in-plane anisotropy. The problem for an arbitrary magnetization direction can be solved numerically.

The studied film contained a relative volume of a ferromagnetic material of 74.5 at.%, which unambiguously exceeds the percolation threshold. However, the magnetization reversal curves show that the film had attributes typical of a film with perpendicular anisotropy. This result was confirmed by the results of transmission electron microscopy obtained for the same film [21]. The peculiarities of the hysteresis sections in the  $M(H_e)$  curves for the film concerned allowed us to substantiate, in work [21], the statement that, in the magnetic aspect, the examined film is biphasic; i.e. it includes a ferromagnetic material (Co), some fraction of which forms a large percolation cluster, and the other fraction consists of electrically insulated metallic ferromagnetic granules. A rather large granular fraction of the film (non-percolating granules) may probably originate from the fact that Co granules have insulating oxide shells, which prohibit them from contact with one another. However, a smaller fraction of granules form a large percolation cluster. The model is developed taking into account that the film has another magnetic component.

In addition, some specific data for the studied film are obtained. The data testifying to its biaxial character are most interesting. The biaxial character of the film may probably result from the used technology of its fabrication under the conditions of the inclined sputtering on areas with a high content of the magnetic component.

*The work was partially supported by the State Fund for Fundamental Researches of Ukraine in the framework of the program “Fundamental problems of nanostructural systems, nanomaterials, and nanotechnologies” (project 1/14-H).*

1. W. Hao, M. Sun, H. Xu, and T. Wang, in *Proceedings of the 3-rd Intern. Nanoelectronic Conference INEC'2010* (IEEE, 2010), p. 1173.
2. Z.W. Liu, Y. Liu, Y.G. Ma, C.Y. Tan, and C.K. Ong, *J. Magn. Magn. Mater.* **313**, 37 (2007).
3. J.C. Sohn, D.J. Byun, and S.H. Lim, *J. Magn. Magn. Mater.* **272**, 1500 (2004).
4. C.H. Schwalb, C. Grimm, M. Baranowski, R. Sachser, F. Porrati, H. Reith, P. Das, J. Müller, F. Völklein, A. Kaya, and M. Huth, *Sensors* **10**, 9847 (2010).

5. R.H. Victora and Xiao Shen, *Proc. IEEE* **96**, 1799 (2008).
6. A. Glatz, I.S. Beloborodov, and V.M. Vinokur, *Europhys. Lett.* **82**, 47002 (2008).
7. C. Kittel, *Phys. Rev.* **70**, 965 (1946).
8. L Néel, *C.R. Acad. Sci.* **224**, 1488 (1947).
9. S.V. Vonsovsky, *Magnetism* (Wiley, New York, 1974).
10. V.M. Kalita and S.M. Ryabchenko, *Fiz. Nizk. Temp.* **38**, 253 (2012).
11. A.A. Timofeev, S.M. Ryabchenko, A.F. Lozenko, and P.A. Trotsenko, *Fiz. Nizk. Temp.* **33**, 1282 (2007).
12. S.M. Ryabchenko, A.A. Timofeev, V.M. Kalita, A.F. Lozenko, P.A. Trotsenko, V.A. Stefanovich, and M. Munakata, *Fiz. Nizk. Temp.* **36**, 861 (2010).
13. S. Bedanta, J. Rhensius, W. Kleemann, P. Parashar, S. Cardoso, and P.P. Freitas, *J. Appl. Phys.* **105**, 07C306 (2009).
14. D. Bisero, E. Angeli, F. Spizzo, P. Vavassori, and F. Ronconi, *J. Magn. Magn. Mater.* **262**, 116 (2003).
15. M.A. Chuev, *JETP Lett.* **85**, 611 (2007).
16. A.A. Timopheev, S.M. Ryabchenko, V.M. Kalita, A.F. Lozenko, P.A. Trotsenko, V.A. Stephanovich, A.M. Grishin, and M. Munakata, *J. Appl. Phys.* **105**, 083905 (2009).
17. I.M. Mryglod and V.V. Sokolov, *Ukr. J. Phys.* **54**, 501 (2009).
18. O.V. Stognei, A.V. Sitnikov, Yu.E. Kalinin, S.F. Avdeev, and M.N. Kopytin, *Fiz. Tverd. Tela* **49**, 158 (2007).
19. V.M. Kalita, A.F. Lozenko, S.M. Ryabchenko, A.V. Los, A.V. Sitnikov, and O.V. Stognei, *J. Phys. Condens. Matter* **25**, 066009 (2013).
20. C. Grimaldi, *Phys. Rev. B* **89**, 214201 (2014).
21. M.M. Kulyk, V.M. Kalita, A.F. Lozenko, S.M. Ryabchenko, O.V. Stognei, A.V. Sitnikov, and V. Korenivski, *J. Phys. D* **47**, 345002 (2014).
22. A.A. Timofeev, S.M. Ryabchenko, V.M. Kalita, A.F. Lozenko, P.A. Trotsenko, O.V. Stognei, and A.V. Sitnikov, *Fiz. Tverd. Tela* **53**, (2011).
23. V.M. Kalita, A.A. Timopheev, A.F. Lozenko, S.M. Ryabchenko, A.V. Los, O.V. Stognei, and A.V. Sitnikov, *J. Appl. Phys.* **110**, 113918 (2011).

Received 23.09.14.

Translated from Ukrainian by O.I. Voitenko

*M.M. Кулик, В.М. Калита,  
А.Ф. Лозенко, С.М. Рябченко,  
О.В. Стогней, А.В. Ситніков*

ВПЛИВ ВНУТРІШНЬОПЛОЩИННОЇ  
АНІЗОТРОПІЇ НА ВЕЛИЧИНУ ПОЛЯ КРИТИЧНОГО  
ПЕРЕХОДУ В НАНОГРАНУЛЯРНИХ ПЛІВКАХ  
З ПЕРПЕНДИКУЛЯРНОЮ АНІЗОТРОПІЄЮ

Резюме

Досліджено вплив внутрішньоплощинної анізотропії на намагнічування наногранулярної плівки з перпендикулярною

анізотропією. Показано, що в нахиленому до нормалі плівки магнітному полі спостерігається критичний перехід від неоднорідного магнітного стану гранул з неколінеарним напрямком їх моментів до однорідного стану з паралельною орієнтацією магнітних моментів гранул. Отримано, що внутрішньоплощинна анізотропія впливає на кутову залежність критичного поля. Теоретичний опис орієнтованого ансамблю двовісних частинок проведено в наближенні двоїмого потенціалу. Незважаючи на двовісність магнітної анізотропії частинок, у неоднорідному стані, ансамбль розбивається на два підансамблі, у кожному з яких магнітні

моменти частинок співнаправлені. У критичному полі відбувається перехід від неоднорідного стану із двома підансамблями до однорідного стану. Дані розрахунків порівняні з результатами дослідження наногранулярної плівки  $\text{Co}/\text{Al}_2\text{O}_n$ , з перпендикулярною анізотропією, яка містить 74,5 ат.% Co, що перевищує поріг перколяції. Магнітний момент такої плівки складається із суми двох внесків: наногранулярного із двовісною анізотропією гранул і фази, що утворює перколяційний кластер. Магнітні властивості виділеного із загальної намагніченості наногранулярного внеску добре узгоджуються з даними розрахунків.